

# Supporting Information

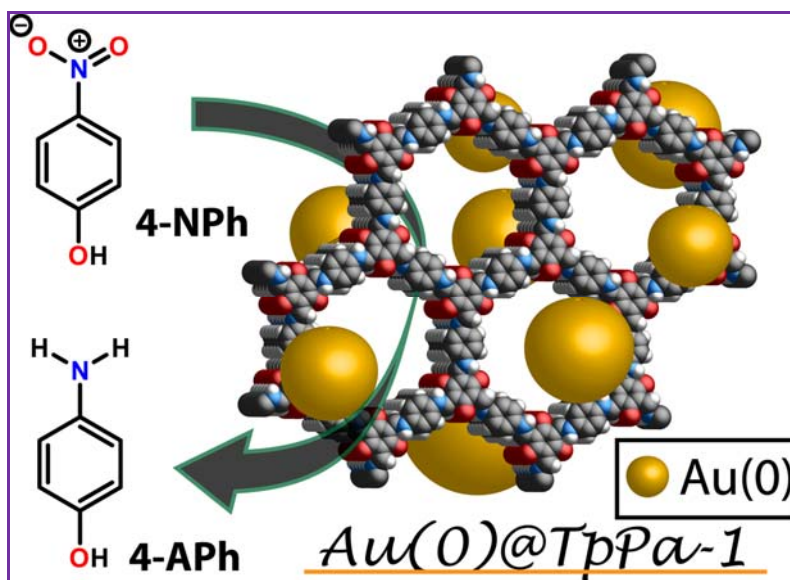
## Highly Stable Covalent Organic Framework-Au Nanoparticles Hybrids for Enhanced Activity for Nitrophenol Reduction

Pradip Pachfule,<sup>a</sup> Sharath Kandambeth,<sup>a</sup> David Díaz Díaz,<sup>b,c</sup> and Rahul Banerjee<sup>a\*</sup>

<sup>a</sup> Physical/Materials Chemistry Division, CSIR-National Chemical Laboratory, Dr. Homi Bhabha Road, Pune-411008, India.

E-mail: [r.banerjee@ncl.res.in](mailto:r.banerjee@ncl.res.in)

<sup>b,c</sup> Institut für Organische Chemie, Universität Regensburg, Universitätsstr. 31, 93053 Regensburg (Germany) and IQAC-CSIC (Spain).



## Contents List

<b>Section S1.</b> Experimental procedures, materials and methods	<b>3</b>
<b>Section S2.</b> Synthesis and characterization of <b>TpPa-1</b>	<b>5</b>
<b>Section S3.</b> Synthesis and characterization of <b>Au(0)@TpPa-1</b>	<b>8</b>
<b>Section S4.</b> General procedures followed for nitrophenol reduction and catalytic conversions by <b>Au(0)@TpPa-1 (1.20 wt%)</b> , <b>Au(0)@TpPa-1 (2.20 wt%)</b> , <b>HAuCl<sub>4</sub>·3H<sub>2</sub>O</b>	<b>16</b>
<b>Section S5.</b> Catalyst leaching and recyclability tests	<b>22</b>
1. Au leaching test	22
2. Catalyst recyclability experiments	23
(a). Optical and SEM images of as synthesized and recycled <b>Au(0)@TpPa-1</b> catalysts	
(b). TEM images of as synthesized and recycled <b>Au(0)@TpPa-1</b> catalysts	
<b>Section S6.</b> Thermogravimetric analyses of <b>Au(0)@TpPa-1</b>	<b>25</b>
<b>Section S7.</b> Comparison of rate constant for <b>Au(0)@TpPa-1</b> with literature reported Au-based catalysts for nitrophenol reduction reactions	<b>26</b>

## Section S1. Experimental procedures, materials and methods:

All the reagents and solvents used for the synthesis of **TpPa-1**, **Au(0)@TpPa-1** and nitro reduction reaction were commercially available and used as received. The gold salt used **HAuCl<sub>4</sub>·3H<sub>2</sub>O** for the synthesis of **Au(0)@TpPa-1** was purchased from Alfa Aesar. 4-nitrophenol and Sodium borohydride used for catalysis were purchased from Sigma Aldrich.

### **FT-IR, PXRD, SEM, EDAX, TEM, TGA and NMR analyses:**

Fourier transform infrared (FT-IR) spectra were taken on a Bruker Optics ALPHA-E spectrometer with a universal Zn-Se ATR (attenuated total reflection) accessory in the 600-4000 cm<sup>-1</sup> region or using a Diamond ATR (Golden Gate). Powder X-ray diffraction (PXRD) patterns were recorded on a Phillips PANalytical diffractometer for Cu K $\alpha$  radiation ( $\lambda$  = 1.5406 Å), with a scan speed of 1° min<sup>-1</sup> and a step size of 0.02° in  $2\theta$ . SEM images were obtained with a Zeiss DSM 950 scanning electron microscope and FEI, QUANTA 200 3D. Scanning Electron Microscope with tungsten filament as electron source operated at 10 kV was used to get SEM images. The samples were sputtered with Au (nano-sized film) prior to imaging by a SCD 040 Balzers Union as well as by sprinkling the powder on carbon tape. Microscopy analyses were performed using a LEICA Stereoscan 440 scanning electron microscope (SEM) equipped with Phoenix energy dispersive analysis of X-ray (EDAX). To investigate the microstructure and morphology of the nanoparticles, we used the FEI (model Tecnai F30) high resolution transmission electron microscope (HRTEM) equipped with field emission source operating at 300 KeV to image the nano-crystals on carbon-coated copper TEM grids. The nanoparticles were dispersed in iPrOH and drop casted on the TEM grids. Thermogravimetric analyses (TGA) were carried out on a TG50 analyzer (Mettler-Toledo) or a SDT Q600 TG-DTA analyzer under N<sub>2</sub> and air atmosphere at a heating rate of 10 °C min<sup>-1</sup> within a temperature range of 30-900 °C). NMR data were taken on Bruker 200 and 400 MHz NMR spectrometers.

**N<sub>2</sub> adsorption isotherms and pore size distribution measurements:**

Autosorb-iQ automatic volumetric instrument has been used for low pressure volumetric N<sub>2</sub> gas adsorption measurements involved in this work, performed at 77 K maintained by a liquid nitrogen bath, with pressures ranging from 0 to 760 Torr. Ultra high-purity N<sub>2</sub> was obtained by using calcium aluminosilicate adsorbents to remove trace amounts of water and other impurities before introduction into the system. For the gas adsorption studies of **TpPa-1**, the solvent exchanged sample was dried under a dynamic vacuum ( $<10^{-3}$  Torr) at room temperature (RT) overnight followed by heating at 100 °C for 12 h and 120 °C for 12 h under a dynamic vacuum. The completely dried samples (70 mg) were loaded for gas adsorption study in the sample cells. The as synthesized sample of **Au(0)@TpPa-1** was used for the N<sub>2</sub> adsorption isotherm studies and pore sized distributions plots were calculated using Quenched Solid Density Functional Theory (QSDFT) and Density Functional Theory (DFT) methods using the nitrogen adsorption isotherms obtained at 77 K and 1 atm pressure.

**Inductively coupled plasma (ICP) Analysis:**

The weight percentage loading of Au on TpPa-1 COF in **Au(0)@TpPa-1** has been analyzed using Inductively Coupled Plasma Optical Emission Spectrometry (ICP-OES) instrument from **Spectro Arcos (Model No.: ARCOS-FHS-12; Input: 230 VAC 50/60 Hz; Part No.: 76004554)**. The sample for ICP analyses were prepared by using Aqua regia as a digesting solution. In a typical stock solution preparation, 4 mg of **Au(0)@TpPa-1** was dissolved in 10 ml Aqua regia with sonication for 15 min. After complete dissolution of catalyst into Aqua regia solution, the stock solution was filtered through Syringe filters (0.22 μ) in order to remove the insoluble impurities if any. The stock solution was further diluted with water to ppm level accordingly.

## Section S2. Synthesis and characterization of TpPa-1:

### Synthesis of TpPa-1:

The synthesis of **TpPa-1** was performed according to the literature reported our recent communication.<sup>2</sup> Specifically, a pyrex tube (o.d.  $\times$  i.d. = 10  $\times$  8 mm<sup>2</sup> and length 18 cm) was charged with triformylphloroglucinol (**Tp**) (63 mg, 0.3 mmol), paraphenylenediamine (**Pa-1**) (48 mg, 0.45 mmol), mesitylene (1.5 mL), dioxane (1.5 mL), and aqueous acetic acid (0.5 mL from a 3 M solution). The mixture was sonicated for 10 minutes in order to get a homogenous dispersion. The tube was then flash frozen at 77 K (liquid N<sub>2</sub> bath) and degassed by three freeze-pump-thaw cycles. The tube was sealed off and heated at 120 °C for 3 days. A red colored precipitate formed was collected by centrifugation or filtration and washed with anhydrous acetone. The powder collected was then solvent exchanged with anhydrous acetone 5-6 times and then dried at 180 °C under vacuum for 24 h to give the product as a deep red colored powder in 80% isolated yield (89 mg).

**IR (powder, cm<sup>-1</sup>):** 1589 (s), 1578 (w), 1456 (s), 1255 (s), 1089 (m), 998 (s), 830 (s)

**Elemental analysis.** For C<sub>80</sub>O<sub>12</sub>N<sub>13</sub>H<sub>48</sub>

Calculated: **C**, 69.5; **H**, 3.47; **N**, 13.87

Found: **C**, 69.1; **H**, 4.01; **N**, 14.22

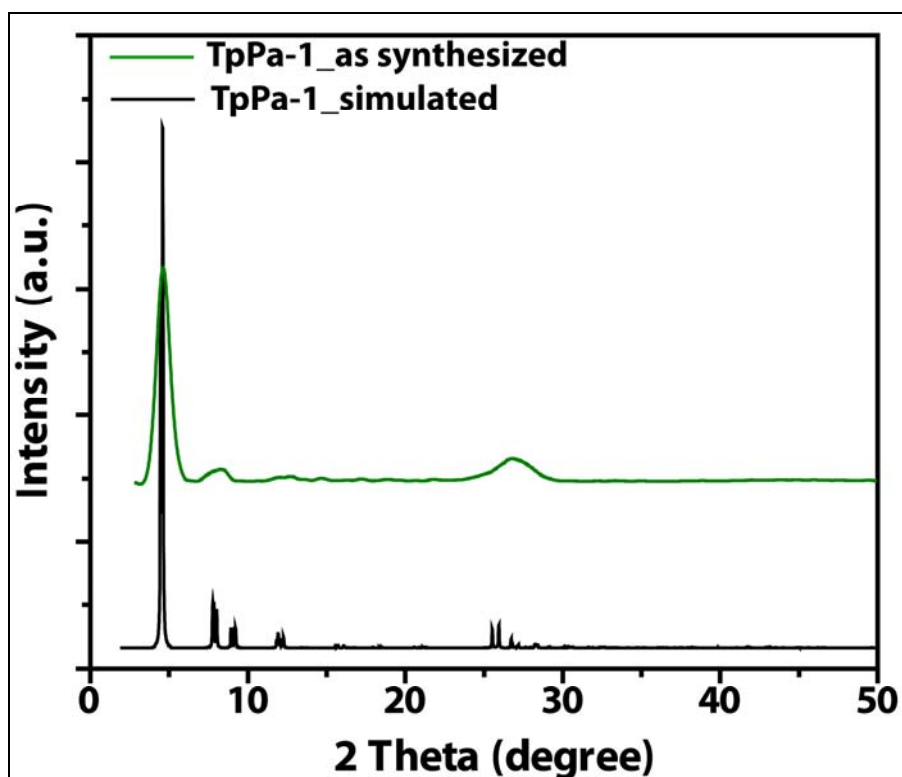


**Figure S1.** XRD pattern observed for *TpPa-1* and its comparison with the corresponding simulated pattern, showing peak to peak match with the bulk material.

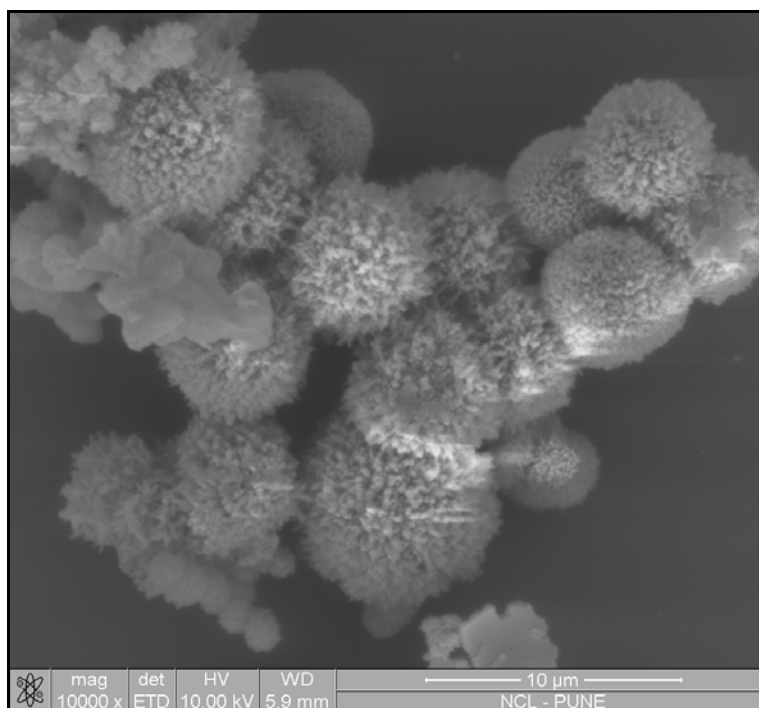


**Figure S2.** SEM image of the *TpPa-1* showing distinct flower-like morphology.

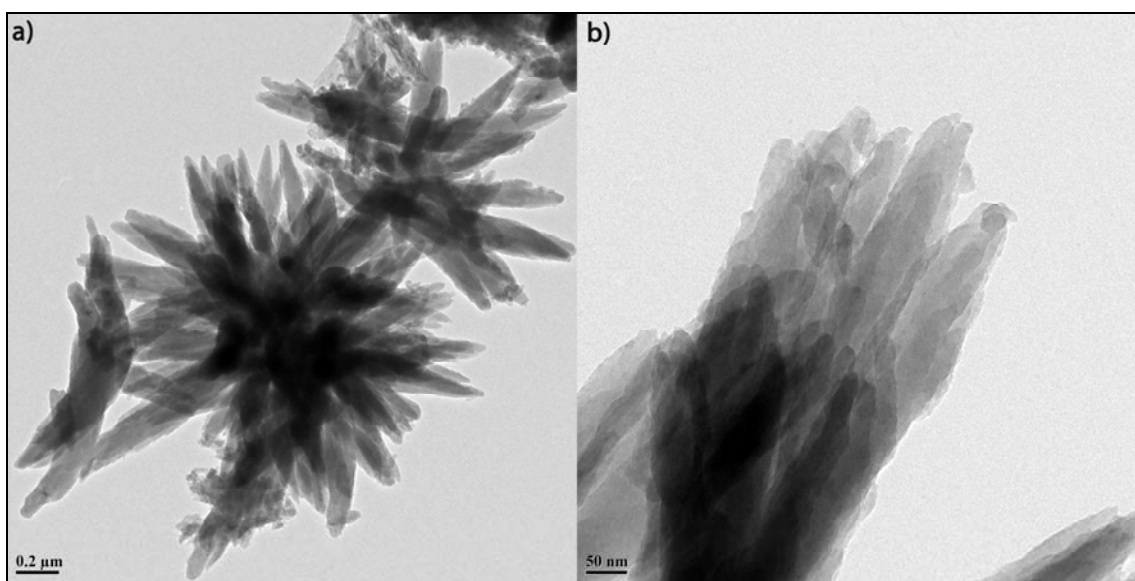


**Figure S3.** Low resolution TEM images of **TpPa-1**. a) TEM image of **TpPa-1** showing flower like morphology of COF. b) High resolution TEM image of **TpPa-1** showing sheets like structures arranged in lamellar fashion.

### Section S3. Synthesis and characterization of Au(0)@TpPa-1:

The Au(0) doped **TpPa-1** catalyst, **Au(0)@TpPa-1** was synthesized by the desperation of pre-synthesized and activated **TpPa-1** (98.5 mg) in 5 mL of MeOH under ambient conditions, to which a MeOH solution (2 mL) containing H<sub>2</sub>AuCl<sub>4</sub>·3H<sub>2</sub>O (1.5 mg, 0.005 mmol) was added drop wise under vigorous stirring. The mixture was evaporated until it becomes mushy. To this solution, 2 mL MeOH was subsequently added into the slurry, followed by a solution (2 mL) of NaBH<sub>4</sub> (0.5 mmol in MeOH) under vigorous stirring. After 30 min, the residue was recovered by filtration and thoroughly washed with MeOH (3 × 10 mL) to remove any impurity. The so prepared sample of **Au(0)@TpPa-1** was further dried in a vacuum drying oven at 50 °C.

**IR (powder, cm<sup>-1</sup>):** 1578 (s), 1561(w), 1439 (s), 1258 (s), 1101 (m), 991 (s), 832 (s)

**Elemental analysis.** For *Au(0)@TpPa-1* [98.5 % TpPa-1 + 1.5 % Au(0)]

Calculated: **C**, 68.45; **H**, 3.41; **N**, 13.66

Found: **C**, 67.11; **H**, 3.25; **N**, 14.57



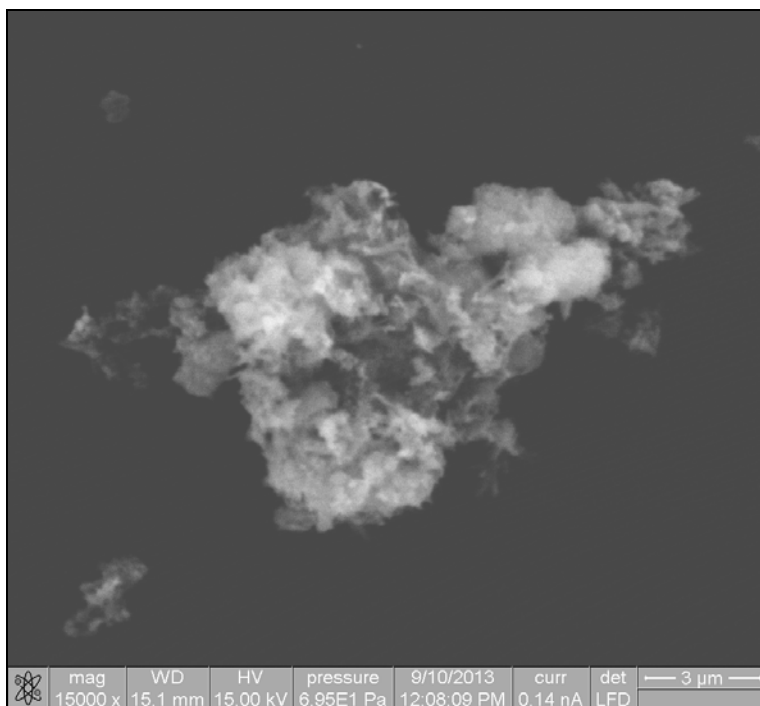


**Figure S4.** SEM image of the  $\text{Au}(0)@\text{TpPa-1}$  showing the morphology of the ***TpPa-1*** after incorporation of  $\text{Au}(0)$  nanoparticles.

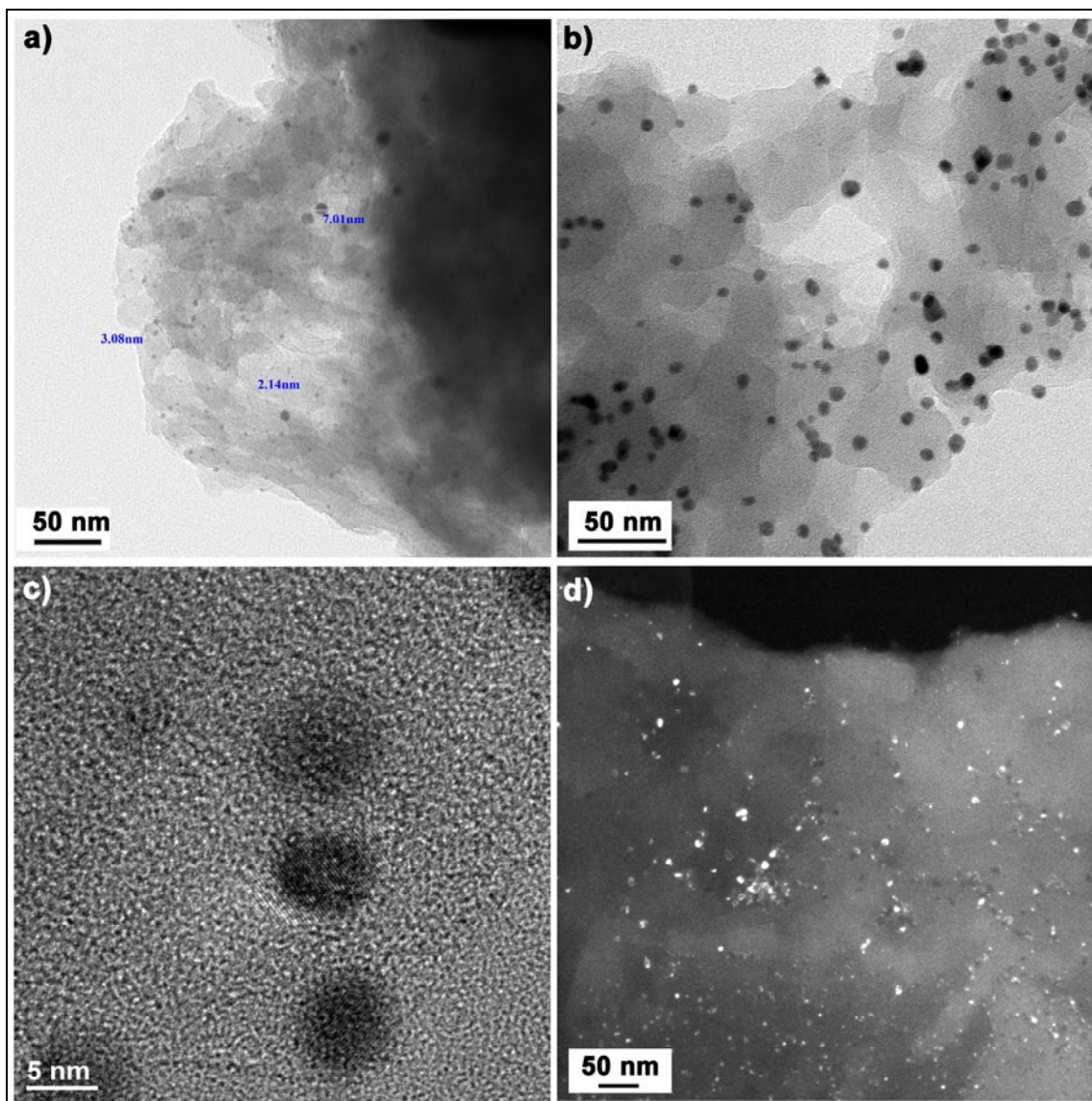


**Figure S5.** High and low resolution TEM images of **Au(0)@TpPa-1**. a) Low resolution TEM image shows finely distributed  $5 \pm 3$  nm sized Au(0) nanoparticles distributed overall **TpPa-1** surface without agglomeration. b) High resolution TEM image of **Au(0)@TpPa-1** showing the uniform distribution of nanoparticles over **TpPa-1** matrix. c) High resolution TEM image of **Au(0)@TpPa-1** showing lattice fringes of Au nanoparticles. d) The 3D distribution of Au(0) nanoparticles within the COF matrix visual from dark field imaging of **Au(0)@TpPa-1** catalyst.

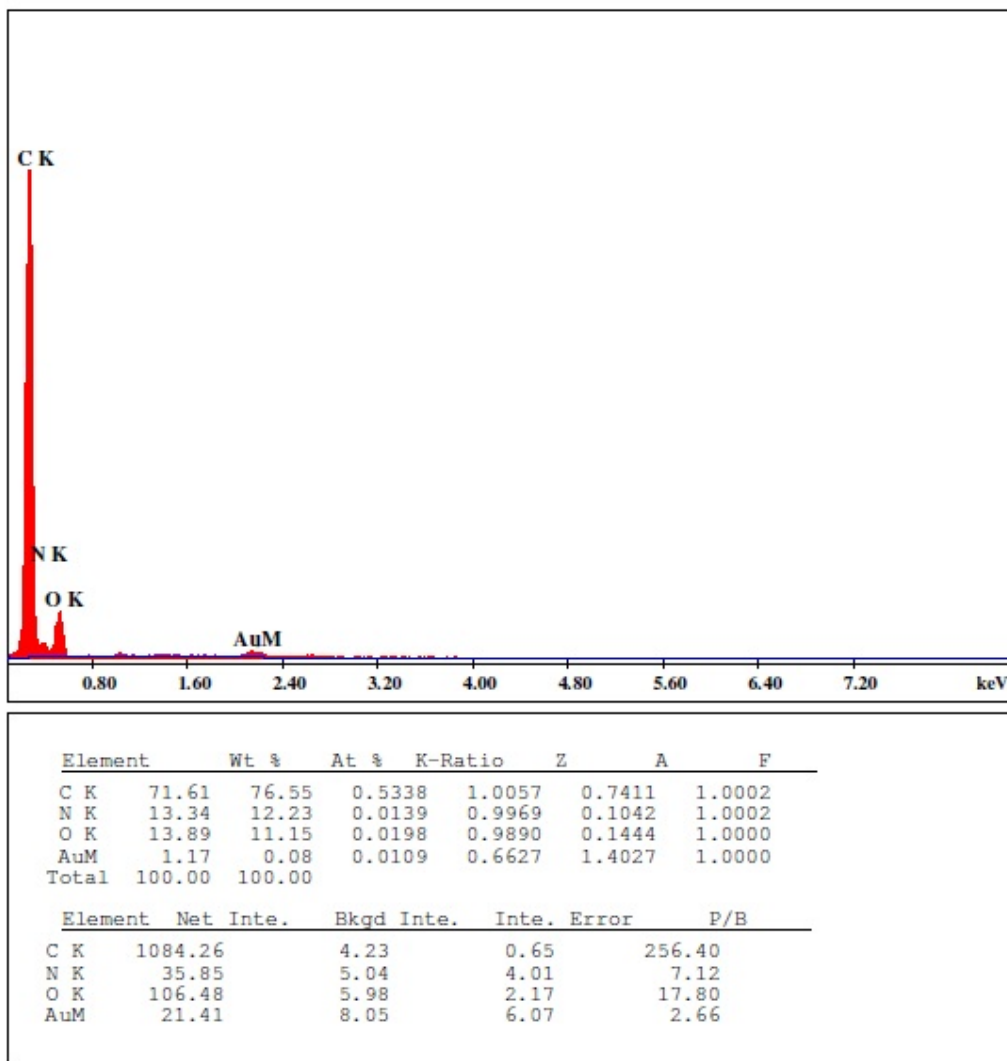


**Figure S6.** EDAX analysis of Au(0)@TpPa-1 showing 1.17 wt% loading of Au(0) nanoparticles.

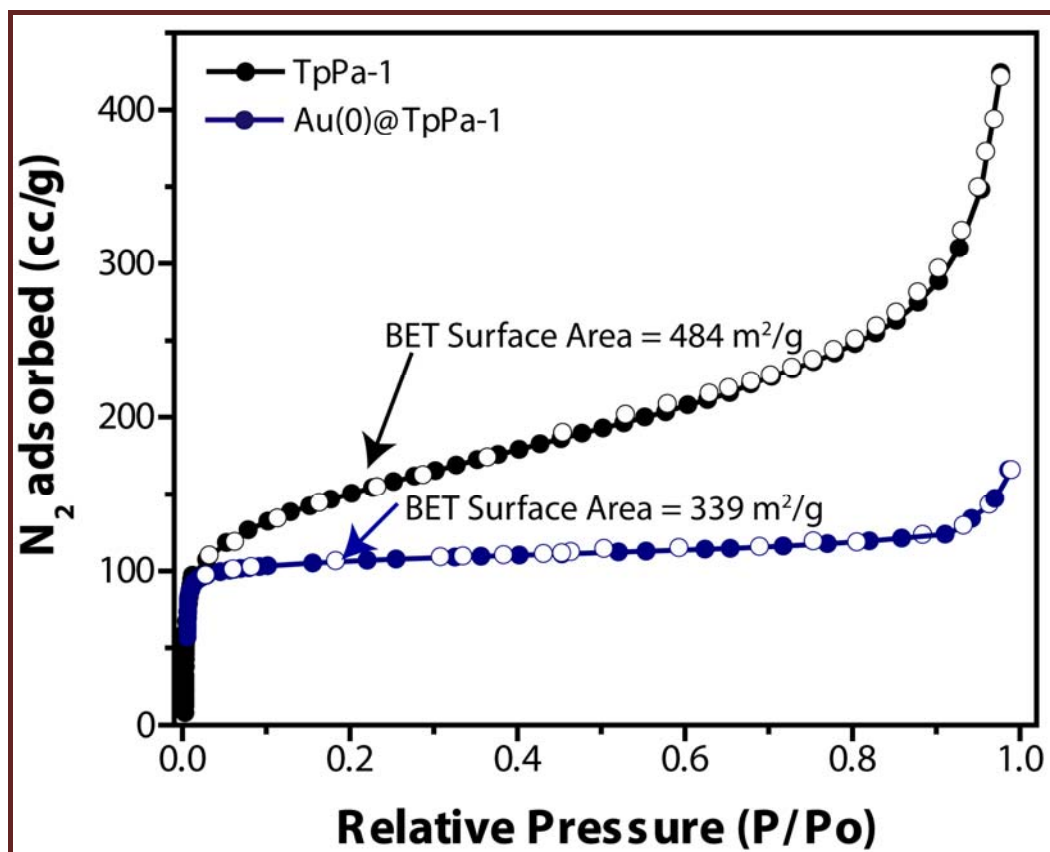


**Figure S7.** N<sub>2</sub> adsorption isotherms for solvent free (evacuated) **TpPa-1** and synthesized catalyst **Au(0)@TpPa-1**. These overall decrease in surface area is justified as loaded nanoparticles occupies the surface (partially or fully) and interlayer spacings in the host COF located at the surface as well as inside the COF matrix.

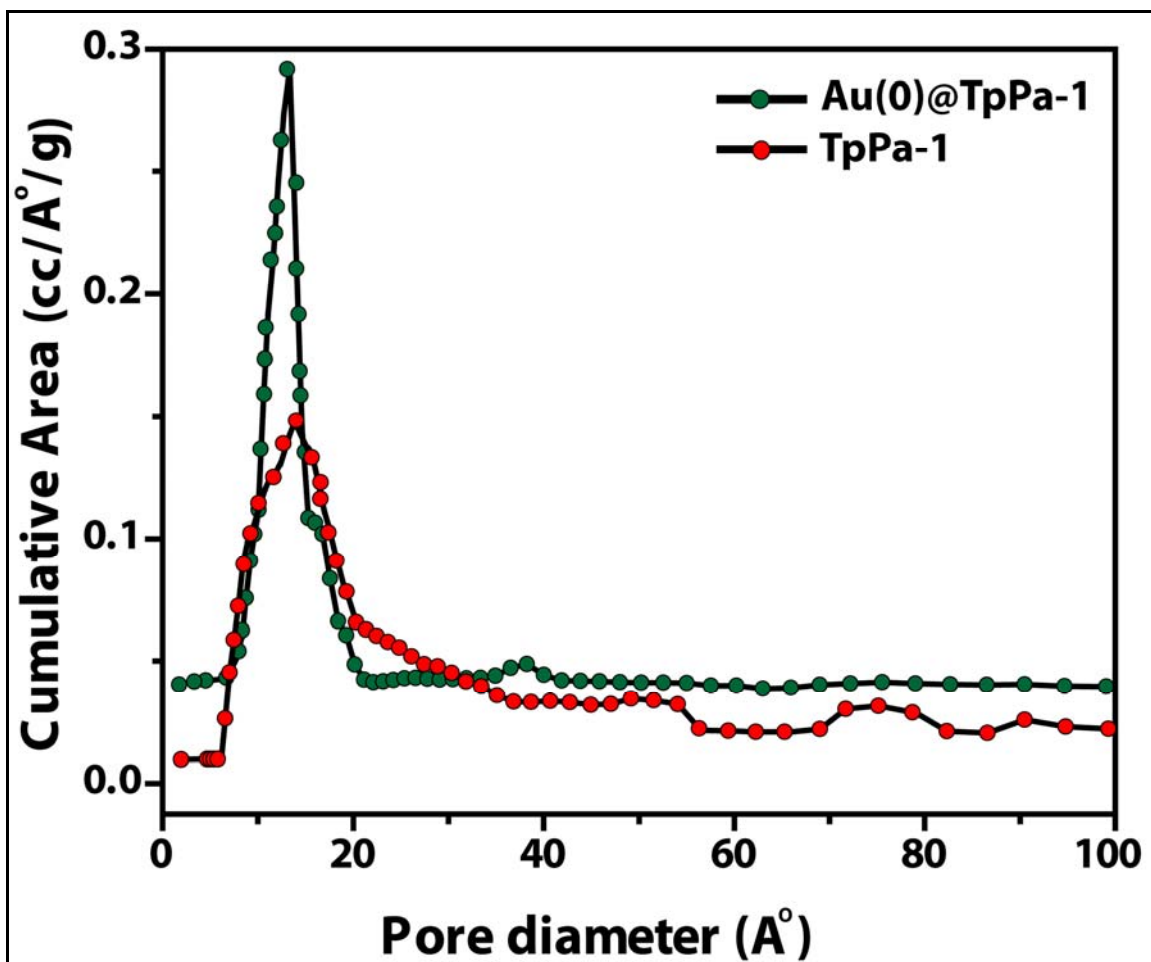


**Figure S8.** Pore size distribution for *Au(0)@TpPa-1* and *TpPa-1* calculated based on collected  $N_2$  isotherms as shown in above figure. The overall decrease in the pore size for *Au(0)@TpPa-1* than *TpPa-1* can be attributed to the loading of nanoparticles within the COF matrix. (Pore size is determined by Density Functional Theory (DFT) pore size distribution method).

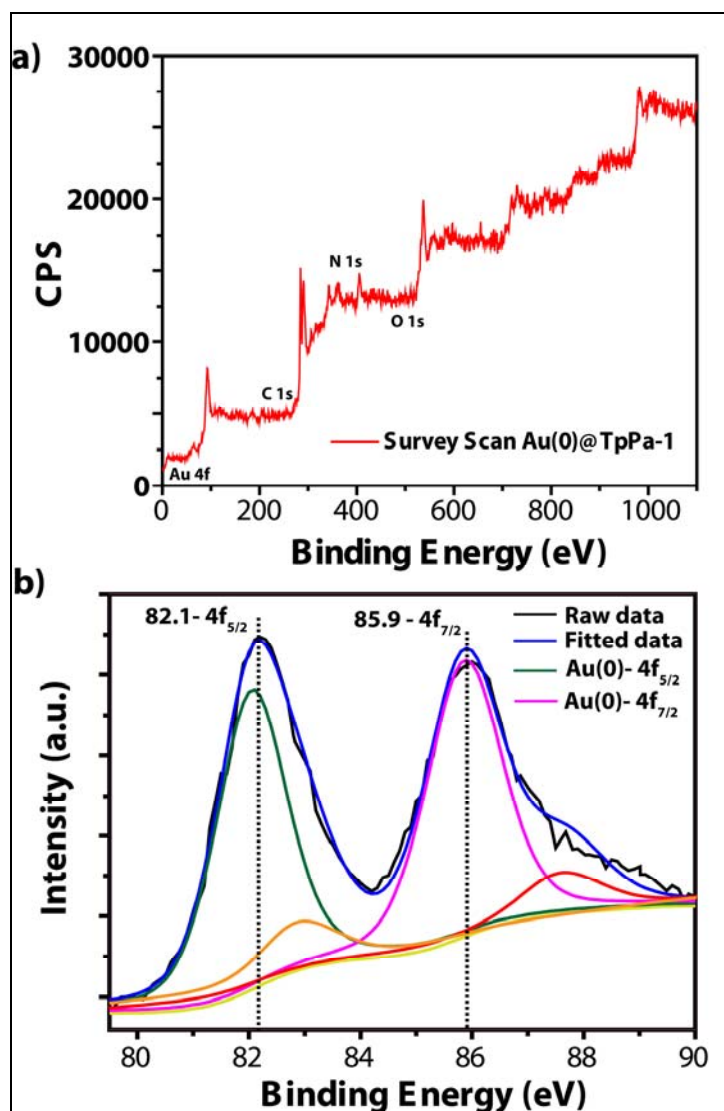


**Figure S9.** XPS analysis of  $\text{Au(0)@TpPa-1}$  sample. a) Survey scan of  $\text{Au(0)@TpPa-1}$  samples showing overall spectra of Au, N, C and O atoms. b) XPS spectrum of the  $\text{Au(0)@TpPa-1}$  in the 4f region showing typical peaks at 82.1 eV ( $4f_{5/2}$ ) and 85.9 eV ( $4f_{7/2}$ ) for Au(0).



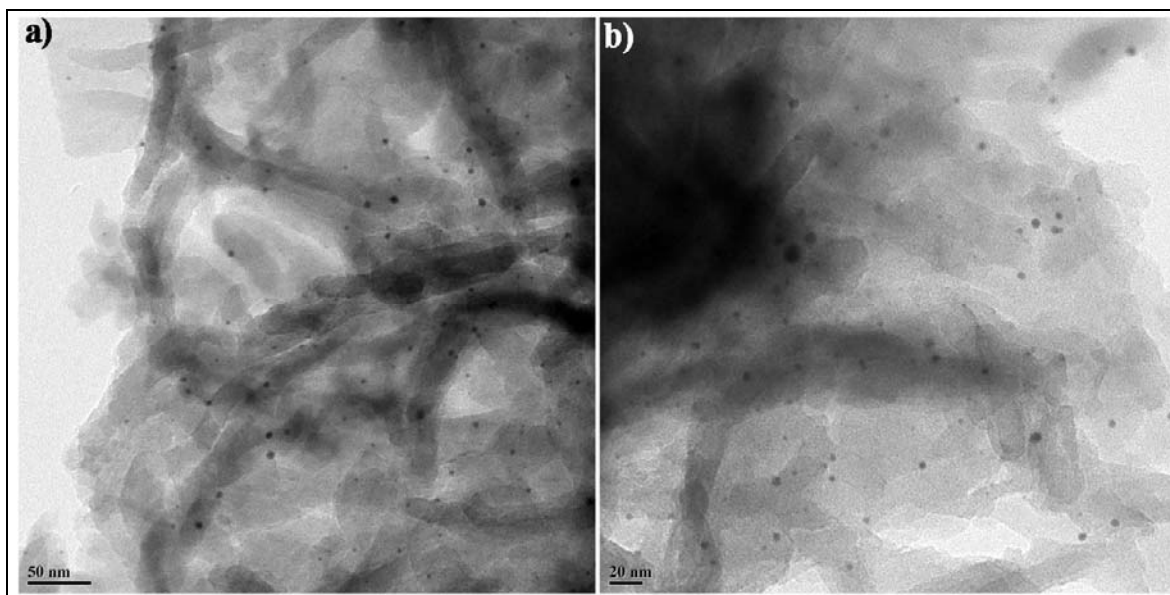


**Figure S10.** TEM images of the  $\text{Au}(0)@\text{TpPa-1}$  catalyst having 0.75 wt% of Au nanoparticles supported on TpPa-1 showing very limited presence of nano-particles, which showed very sluggish kinetics for 4-nitrophenol reduction.

## Section S4. General procedures, characterization and catalytic activities for nitro reduction reaction:

### General procedures for evaluation of catalytic activity of Au(0)@TpPa-1, TpPa-1 and H<sub>2</sub>AuCl<sub>4</sub>·3H<sub>2</sub>O:

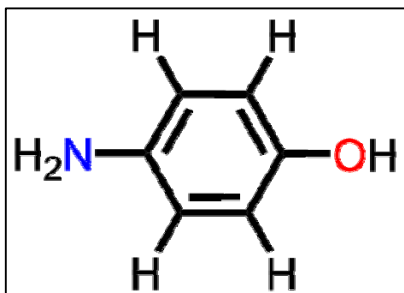
As the nitro reduction reaction is well studied in literature for the confirmation of the catalytic activity of Au based catalysts, we have performed the catalytic transformation reactions using synthesized **Au(0)@TpPa-1** catalyst. The major reasons to choose this reaction as a model reaction are well known mechanism, fast kinetics and room temperature progress of reaction which can be easily monitored by using UV-vis spectroscopy. The reduction of 4-NPh by NaBH<sub>4</sub> was chosen as a model reaction to test the catalytic activity of the **Au(0)@TpPa-1**, **TpPa-1** and **H<sub>2</sub>AuCl<sub>4</sub>·3H<sub>2</sub>O** catalysts.

In a typically reaction for **Au(0)@TpPa-1** catalyst, 162.3 mg of NaBH<sub>4</sub> dispersed in 12 ml distilled water, 15 mL of 0.18 mmol/L 4-NPh was added. To this solution, 20 mg (0.00122 mmol) of catalyst (**Au(0)@TpPa-1**) was added with stirring. After introducing the catalyst, as shown in figure S9 the bright yellow solution gradually faded as the reaction proceeded. The reaction progress was monitored by measuring UV-vis absorption spectra of the mixture. UV-Vis spectra were recorded at short intervals to monitor the progress of the reaction. The absorption spectra of the solution were measured in the range of 250-550 nm. To study the catalyst durability, the catalyst was centrifuged after reaction for 10 minutes, and the clear supernatant liquid was decanted carefully. The catalyst was washed thoroughly with water and methanol, followed by drying at 50 °C for 2 h in vacuum oven. Then, the catalyst was reused for subsequent recycle under the same reaction conditions. The rate constants of the reduction process were determined through measuring the change in absorbance at 400 nm as a function of time.



The similar protocol has been followed to test the catalytic activity of **TpPa-1** and **HAuCl<sub>4</sub>·3H<sub>2</sub>O**, by replacing the **Au(0)@TpPa-1** with mentioned catalysts.

**Characterization of 4-Aminophenol:**



*Off-white solid, 99 % yield*

**Melting point:** 189-192 °C

**<sup>1</sup>H NMR (DMSO-*D*<sub>6</sub>, 200 MHz):** δ 8.30-7.8.28 (s, 1H),  
6.35-6.39 (m, 4H), 4.25-4.27 (s, 2H)

**<sup>13</sup>C NMR (CDCl<sub>3</sub>, 50 MHz):** δ 147.9, 141.5, 116.3

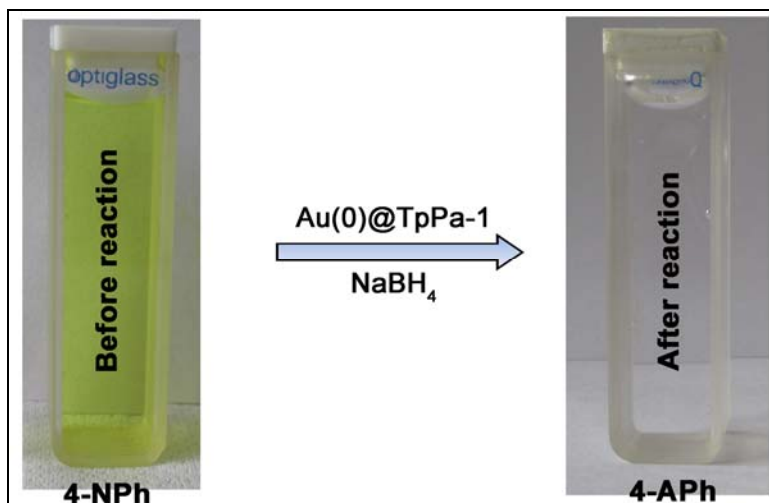


**Figure S11.** The optical images of the color change observed for the conversion of 4-nitrophenol to 4-aminophenol after the addition of **Au(0)@TpPa-1** catalyst after 13 minutes. The catalyst is removed after completion of reaction from the tube containing 4-aminophenol by filtration.

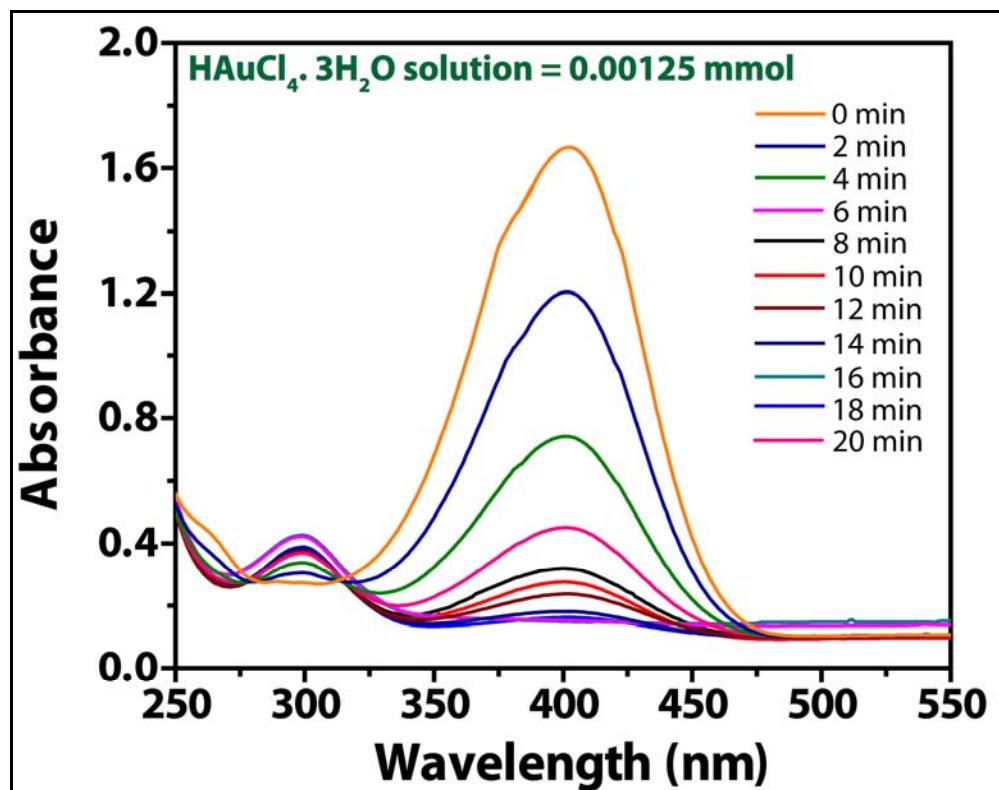


**Figure S12.** Time-dependent evolution of UV-Vis spectra showing complete catalytic reduction of 4-NPh to 4-APh by **HAuCl<sub>4</sub>·3H<sub>2</sub>O** after 20 minutes.

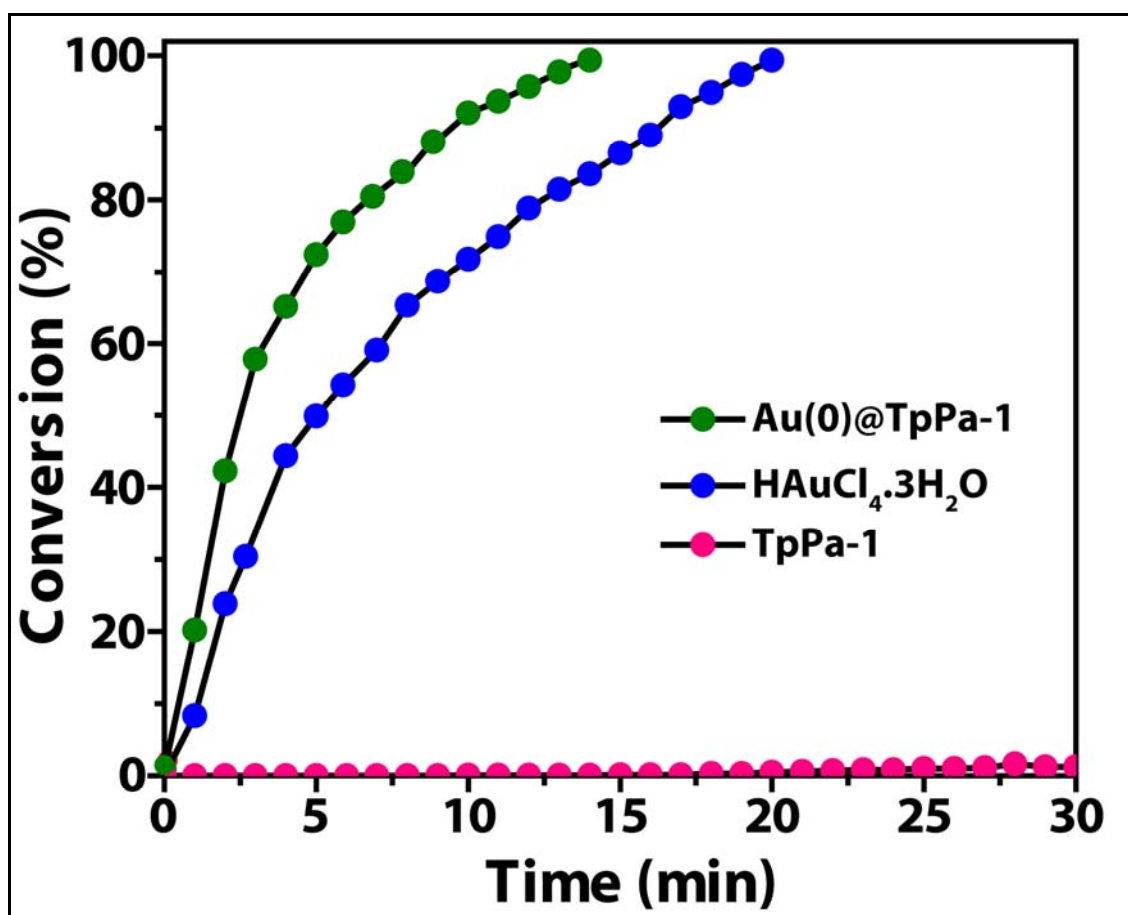


**Figure S13.** Comparative catalytic conversion of 4-NPh over *Au(0)@TpPa-1*, *H[AuCl<sub>4</sub>].3H<sub>2</sub>O* and as synthesized *TpPa-1*. The fast kinetics for nitro reduction is clearly visible in the case of *Au(0)@TpPa-1*.

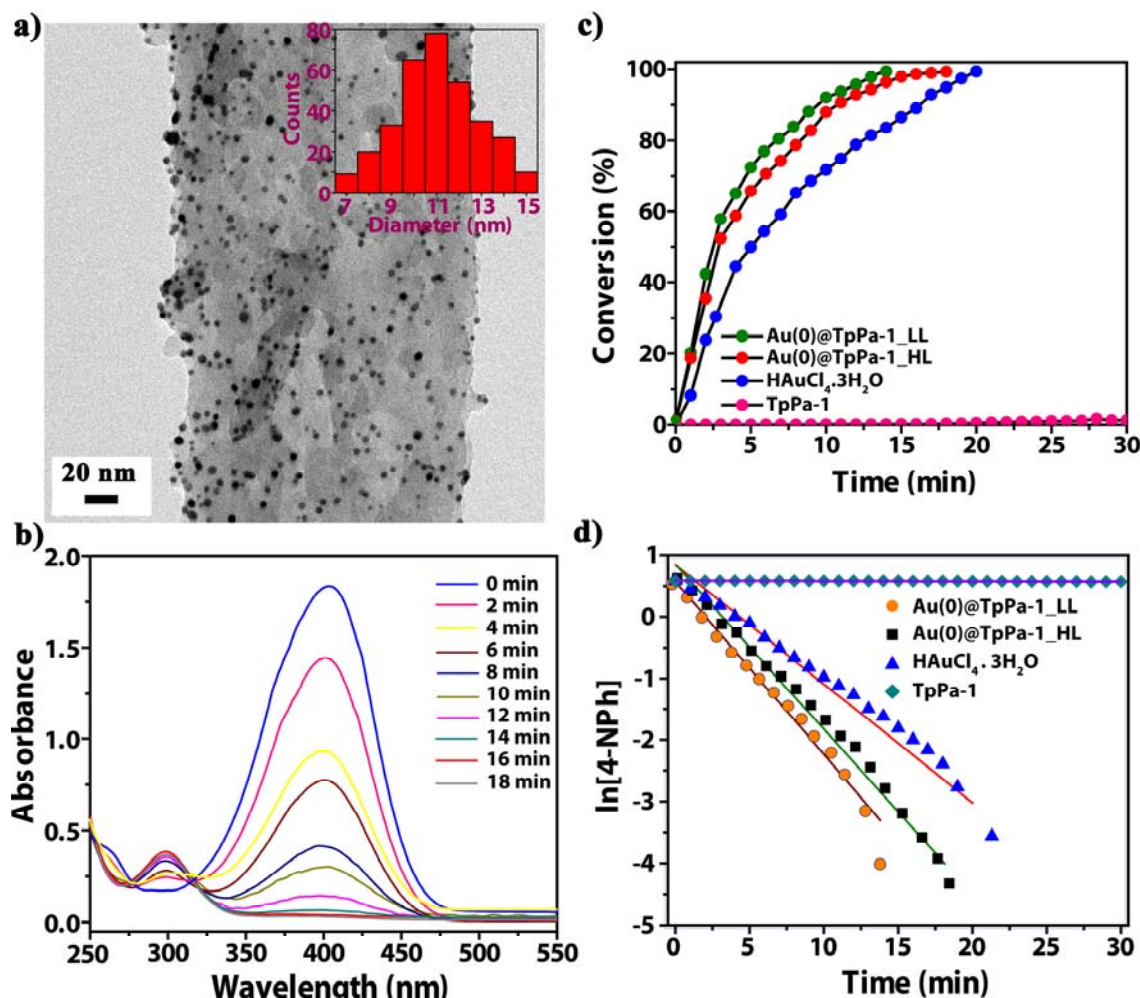


**Figure S14.** TEM and catalytic activity observed for Au(0)@TpPa-1 (2.20 wt% Au loading; Au(0)@TpPa-1\_HL) catalyst. a) Low resolution TEM image of Au(0)@TpPa-1\_HL showing distribution of  $11 \pm 4$  nm sized Au nanoparticles. Inset image: Nanoparticles size distribution histogram. b) Typical time-dependent evolution of UV-Vis spectra showing the catalytic reduction of 4-NPh to 4-Aph by Au(0)@TpPa-1\_HL showing reaction completion within 18 min. c) Comparative catalytic conversion of 4-NPh over Au(0)@TpPa-1\_LL (1.20 wt% Au loading), Au(0)@TpPa-1\_HL, H[AuCl<sub>4</sub>·3H<sub>2</sub>O] and as synthesized TpPa-1. d) Plots of ln[4-NPh] of absorbance of 4-nitrophenol at 400 nm obtained from (b) versus time for the reduction of 4-nitrophenol catalyzed by Au(0)@TpPa-1\_LL, Au(0)@TpPa-1\_HL, H[AuCl<sub>4</sub>·3H<sub>2</sub>O] and as synthesized TpPa-1.

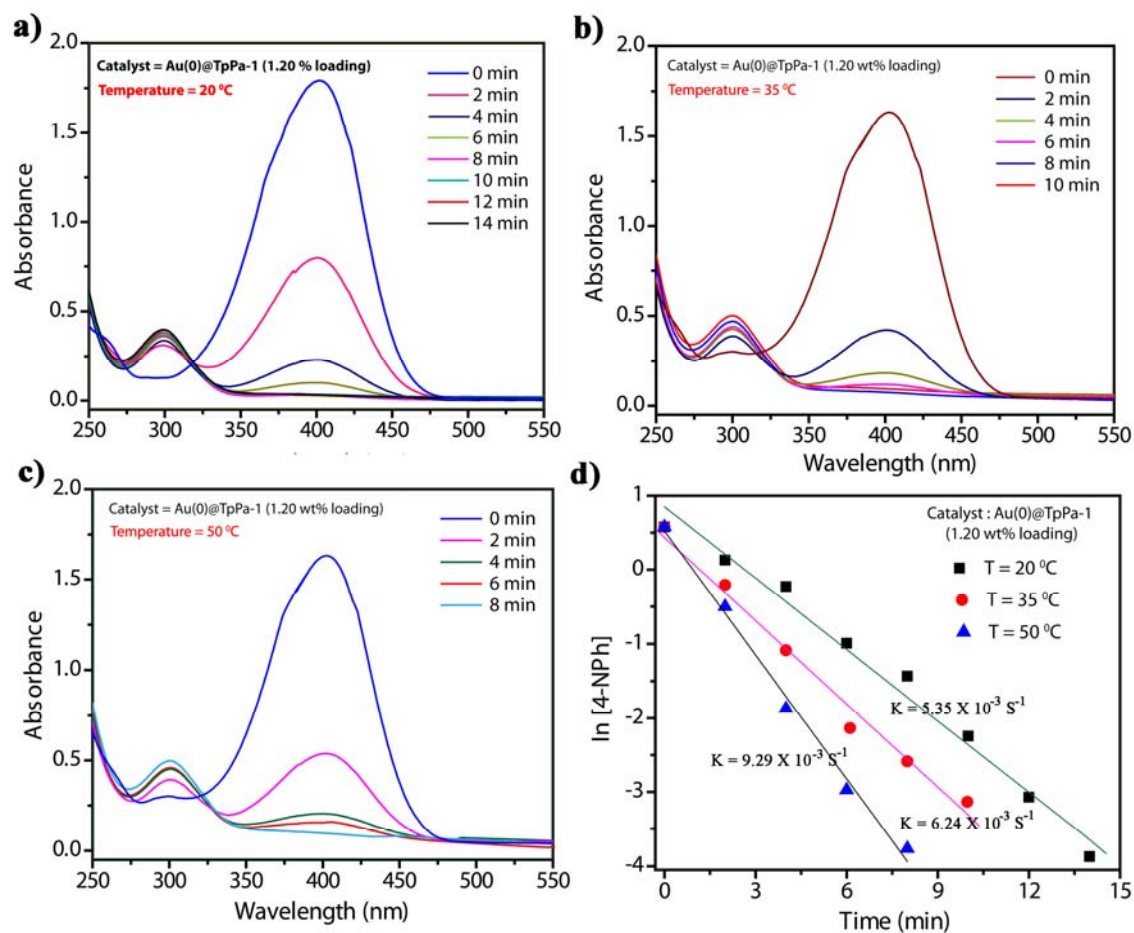


**Figure S15.** Temperature dependant nitrophenol reduction.  $\text{Au}(0)@\text{TpPa-1}$  catalyzed 4-nitrophenol reduction at a) 20 °C, b) 35 °C and c) 50 °C. d) Plots of  $\ln[4\text{-NPh}]$  of absorbance of 4-nitrophenol at 400 nm obtained from (a), (b) and (c) versus time for the reduction of 4-nitrophenol catalyzed by  $\text{Au}(0)@\text{TpPa-1}$  catalyst at various temperatures.

## Section S5. Catalyst leaching and recyclability tests for Au(0)@TpPa-1:

In order to establish the stability and heterogeneity of loaded Au(0) nanoparticles supported on **TpPa-1** for the catalyst **Au(0)@TpPa-1**, the standard leaching experiment was performed:

### 1. Au leaching tests:

In a typical catalyst leaching test experiment, 50 mg of **Au(0)@TpPa-1** catalyst and 4 ml H<sub>2</sub>O was added into a round bottom flask. This catalyst was refluxed for 2 h and filtered in hot conditions into conical flask. To this catalyst free, filtrate solution required amount of the substrates (4-nitrophenol and Sodium borohydride) was added and stirred at room temperature and reaction progress was traced using UV-Vis spectroscopy. The absence of the any trace of product after 30 min reaction confirmed the heterogeneous behavior of the catalyst.

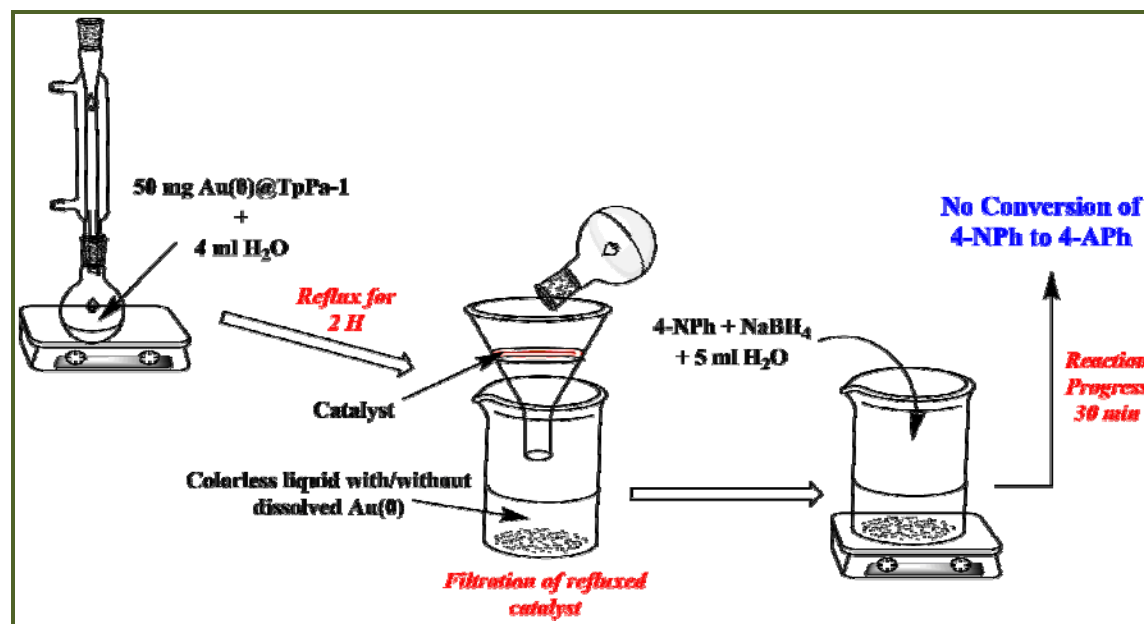


**Figure S16.** Typical catalyst leaching test performed for **Au(0)@TpPa-1** catalyst by refluxing the catalyst in water for 2 h and then following the formation of 4-aminophenol by UV-Vis. The absence of formation of trace of product confirmed the heterogeneous behavior of the catalyst.



## 2. Catalyst recyclability experiments:

### a). Optical and SEM images of Au(0)@TpPa-1 catalysts:

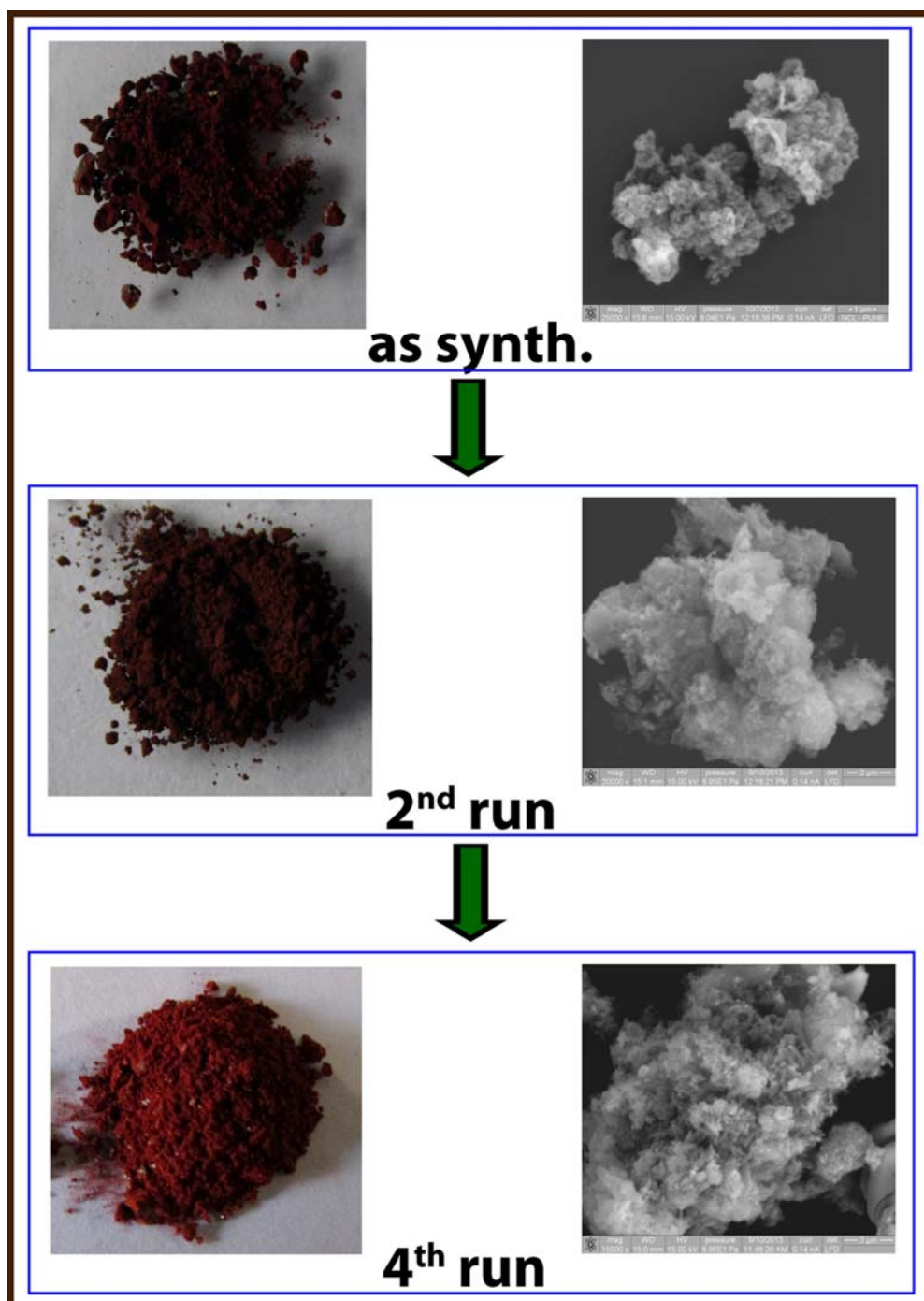


**Figure S17.** Morphological changes observed in Au(0)@TpPa-1 catalyst with increasing number of cycles traced by optical and SEM imaging. The slight changes in color and physical morphology shows the stable behavior of catalyst even after its uses as catalyst.

**b). TEM images of Au(0)@TpPa-1 catalysts:**

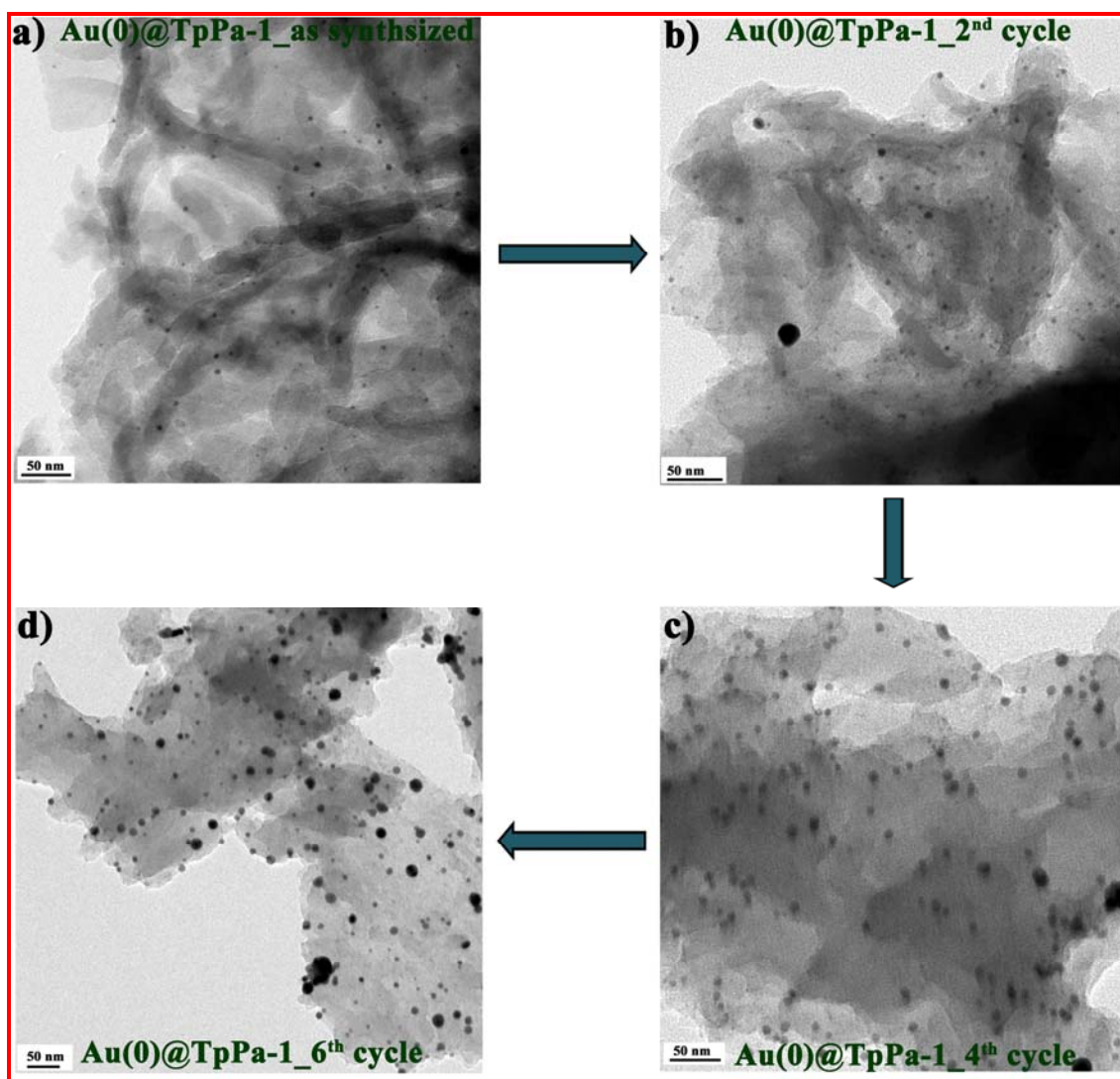


**Figure S14.** The changes in the particle size of doped Au(0) nanoparticles observed with increasing number of catalytic cycles. The partial changes in nanoparticle size traced by TEM imaging shows the high stability of Au(0)@TpPa-1 catalyst after catalytic reaction. The particle size of  $5 \pm 3$  nm observed in as synthesized Au(0)@TpPa-1 catalyst seen to be maintained in good extent after several catalytic cycles also.



**Section S6. Thermogravimetric analyses of Au(0)@TpPa-1:**

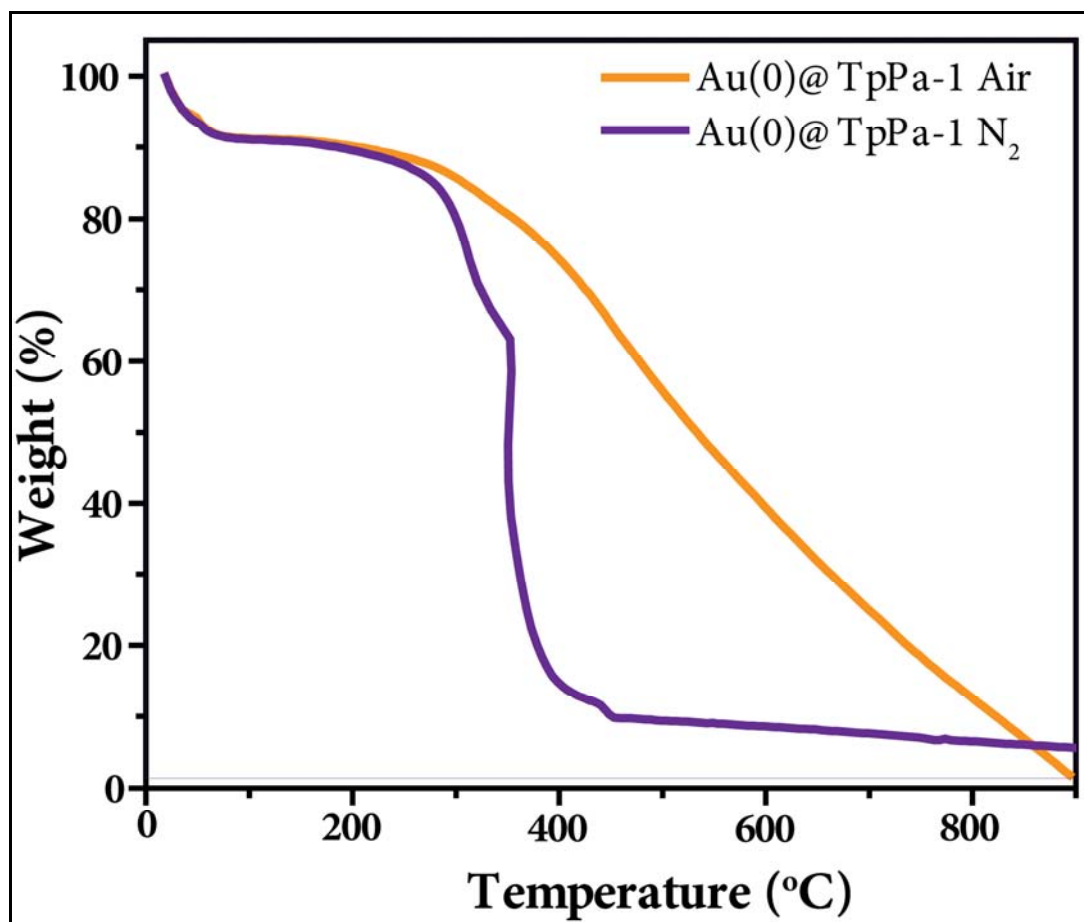


*Figure S15. TGA profiles of Au(0)@TpPa-1 catalyst in nitrogen and air atmosphere.*

**Table S1.** Literature reported rate constants of other similar 4-nitrophenol reduction reactions reported catalyzed using Au-based catalysts:

Sr. No.**	Name of Catalyst	Yield (%)	Time (S)	Rate Constant, k (S <sup>-1</sup> )	Reference
1.	Au/TiO <sub>2</sub>	100	150	$16.9 \times 10^{-3}$	H. Yazid, R. Adnan, and M. A. Farrukh, <i>Indian J. Chem., Sect A</i> , 2013, <b>52A</b> , 184.
2.	Au@SiO <sub>2</sub>	100	1800	$14 \times 10^{-3}$	J. Lee, J. C. Park, and Hyunjoon Song, <i>Adv. Mater.</i> 2008, <b>20</b> , 1523.
3.	Au/Polyaniline	100	300	$11.7 \times 10^{-3}$	J. Han, L. Li and R. Guo, <i>Macromolecules</i> , 2010, <b>43</b> , 10636.
4.	Au/Dendrimer	100	1080	$9.23 \times 10^{-3}$	K. Hayakawa, T. Yoshimura and K. Esumi, <i>Langmuir</i> , 2003, <b>19</b> , 5517.
5.	Au/MgO	98	420	$7.6 \times 10^{-3}$	K. Layek, M. L. Kantam, M. Shirai, D. Nishio-Hamane, T. Sasaki and H. Maheswaran, <i>Green Chem.</i> , 2012, <b>14</b> , 3164.
6	Au(0)@TpPa-1	100	780	$5.35 \times 10^{-3}$	This Work
7.	Au@Ag/MOF	100	900	$4.97 \times 10^{-3}$	H. Jiang, T. Akita, T. Ishida, M. Haruta and Q. Xu, <i>J. Am. Chem. Soc.</i> , 2011, 133.
8.	Au/GO	100	1080	$3.13 \times 10^{-3}$	Y. Zhang, S. Liu, W. Lu, L. Wang, J. Tian and X. Sun, <i>Catal. Sci. Technol.</i> , 2011, <b>1</b> , 1142.
9.	Au/GO	100	1800	$2.07 \times 10^{-3}$	Y. Choi, H. S. Bae, E. Seo, S. Jang, K. H. Park and B.-S. Kim, <i>J. Mater. Chem.</i> , 2011, <b>21</b> , 15431.
10.	Au/Fe <sub>3</sub> O <sub>4</sub>	99	5400 s	-	S. Park, I. S. Lee and J. Park, <i>Org. Biomol. Chem.</i> , 2013, <b>11</b> , 395.

**\*\* The serial numbers given are just for the reference. These are not the actual ranking numbers in all the Au based catalysts for 4-nitrophenol reduction.**